Int. J. Nano Dimens. 6(3): 255-261, Summer 2015
ISSN: 2008-8868

Contents list available at **IJND**

International Journal of Nano Dimension

Journal homepage: *www.IJND.ir*

EPR studies of Cd substituted Mn Zn nanoferrites

C. Venkataraju*
R. Paulsingh

Department of Physics, Karpaga Vinayaga College of Engineering and Technology, Near Madhuranthagam, 603 308, India.

Received 10 April 2014
Received in revised form
23 September 2014
Accepted 29 September 2014

ABSTRACT

Nanoparticles of $Mn_{0.5}Zn_{0.5-x}Cd_xFe_2O_4$ with x varying from x = 0.0 to 0.3 were prepared by wet chemical co-precipitation method. The structural and magnetic properties were studied by using X-Ray Diffraction (XRD), Scanning Electron Microscope (SEM), Transmission Electron Microscopy (TEM) and Electron Paramagnetic Resonance (EPR) technique. The lattice constant increases with increase in Cd content. This increase in the lattice constant is due to larger ionic radii of the Cd^{2+} (0.97 Å) ions as compared to Fe^{3+} (0.64 Å) ions. The intensities of the planes (220) and (440), increases with increasing Cd^{2+} ion concentration. This shows that Cd^{2+} ions occupy tetrahedral A sites and octahedral B sites in the nano dimension against their chemical preference for A site. The line width (ΔH_{pp}) and the g value of the Electron paramagnetic resonance (EPR) signal decreases with increase in the Cd content. The magnetic moment of all the samples up to x = 0.2 calculated from EPR studies are lower when compared to the theoretical values. This lower value of magnetic moment confirms the existence of non collinear magnetic structure arising due to significant amount of spin disorder existing at B site.

Keywords: *Nanostructured materials; Chemical synthesis; Electron paramagnetic resonance (EPR); Magnetic Property; Scanning Electron Microscope (SEM).*

INTRODUCTION

The application of nanoparticles has gained much importance in all the fields of science and technology because of their unique optical, electrical and magnetic properties. Magnetic nanoparticles are widely used in ferro fluid applications, magneto calorific applications, device fabrications, targeted drug delivery and hyperthermia treatments. Ferrite nanoparticles are one of the most attractive materials for these applications. Many methods for synthesizing ferrite nanoparticles has been developed, Wet chemical methods such as Co-precipitation [1, 2], Sol-gel [3], Microemulsion [4] Hydrothermal [5] Citrate precursor [6] and Combustion synthesis method [7] are widely used.

* Corresponding author:
Chidambaram Venkataraju
Department of Physics, Karpaga Vinayaga College of Engineering and Technology, Near Madhuranthagam, 603 308, India.
Tel +91 44 27565486
Fax +9144 27565486
Email cvraju_2k@yahoo.com

Co-precipitation is an attractive method of producing nanoferrites because of increased homogeneity, purity and reactivity. They are relatively simple, low cost and their particle size can be easily controlled.

From several recent literatures it is known that the bulk properties of the ferrites changes as its dimensions are reduced to nanoscale. Manganese Zinc Ferrites are technologically important materials because of their high permeability and low loss. By altering the chemical composition of these ferrites, the physical properties can be changed to suit particular applications. Many work have been carried out by the substitution of Cd ion in the spinel structure of ferrites. Rajesh Iyer *et al*. [8] have synthesized nanosized $Mn_{(1-x)}$ Cd_x Fe_2O_4 by a co-precipitation technique. They have reported the effect of Cadmium substitution on saturation magnetization value. In the present investigation the Electron paramagnetic resonance (EPR) studies of Cd substituted Manganese Zinc Ferrites ($Mn_{0.5}$ $Zn_{(0.5-x)}Cd_x$ Fe_2O_4 with x = 0.0, 0.1, 0.2 and 0.3) are reported.

EXPERIMENTAL

Nanoparticles of $Mn_{0.5}$ $Zn_{(0.5-x)}Cd_x$ Fe_2O_4 with x varying from 0.0 to 0.3 were prepared by co-precipitation method. The materials used were aqueous solution of $MnCl_2$, $ZnSo_4$, $CdCl_2$ and $FeCl_3$ in their respective stoichiometry. They were mixed thoroughly at 80˚ C. This mixture was then transferred immediately into a boiling solution of NaOH at 100˚C. Precipitation takes place and the solution was stirred for about 60 min until the reaction is complete. The pH of the solution was maintained at 12 throughout the reaction. Conversion of metal salts into hydroxides and subsequent transformation of metal hydroxide to nano ferrites takes place. The nanoparticles thus formed were isolated by centrifugation and washed several times with deionized water followed by acetone and then dried at room temperature. The dried powder was grounded thoroughly in a clean agate mortar. The obtained powders were used for various characterization studies. X-Ray Diffraction (XRD) was carried out using a PAN analytical X'pert PRO diffractometer using CuKα as radiation source. Data were collected for every 0.02˚ in the angle range 20˚–70˚ of 2θ. Scanning Electron Microscope (SEM) imaging was carried out using the FEI Quanta FEG 200 (HR-SEM) equipment for the surface morphology analysis. The particle size was determined by subjecting the samples to Transmission Electron Microscopy (TEM) using a Phillips CM20 microscope. Electron Paramagnetic Resonance (EPR) spectra were taken by using a X-band CW EPR (EMX 102.7) spectrometer.

RESULTS AND DISCUSSION

Structural Characterization

The X-Ray Diffraction pattern for the sample $Mn_{0.5}Zn_{(0.5-x)}Cd_x$ Fe_2O_4 (with x= 0.0, 0.1, 0.2 and 0.3) is shown in Figure 1. This diffraction line provides a clear evidence for the formation of ferrite phase in all the samples. The broad XRD line indicates that the ferrite particles are of nano size. All the peaks in the diffraction pattern have been indexed and the refinements of the lattice parameter were done using powder X software. The average crystallite size for each composition was calculated from the full width at half maximum intensity for (311) plain using Scherrer's formula [9]. The values of the lattice parameter were determined by using the following equation.

$$a = \frac{d}{\sqrt{h^2 + k^2 + l^2}} \qquad (1)$$

Where, h. k. l are miller indices. The values of the particle size and lattice constant as deduced from the X-Ray Diffraction are given in Table 1.

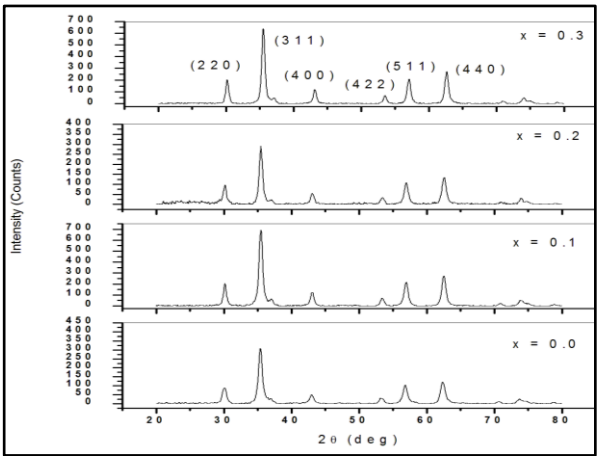

Fig. 1. X-ray Diffraction Pattern for $Mn_{0.5}$ $Zn_{(0.5-x)}Cd_x$ Fe_2O_4 (x = 0.0, 0.1, 0.2, 0.3).

Table 1. Magnetization at an applied field of 20 kOe for the sample $Mn_{0.5}Cd_xZn_{0.5-x}Fe_2O_4$ (with x=0.0, 0.1, 0.2 and 0.3).

X	Composition	Lattice Constant (Å)	Particle Size (nm)	M max (emu/g)	I(220)	I(440)
0.0	$Mn_{0.5}Zn_{0.5}Fe_2O_4$	8.376	14	12.6	110	148
0.1	$Mn_{0.4}Cd_{0.1}Zn_{0.5}Fe_2O_4$	8.382	14	11.2	173	179
0.2	$Mn_{0.3}Cd_{0.2}Zn_{0.5}Fe_2O_4$	8.412	13.6	6.5	221	177
0.3	$Mn_{0.2}Cd_{0.}3Zn0_{.5}Fe_2O_4$	8.416	13	4.9	122	95

The bulk value of the lattice constant for $Mn_{0.5}Zn_{0.5}Fe_2O_4$ reported in the literature by other method is 8.480 [10]. However in the present investigation, a decrease in the lattice constant is observed. A similar decrease in the lattice constant for $Mn_{0.499}\ Zn_{0.495}\ Fe_{1.99}O_{4\ prepared}$ by co-precipitation method was reported by Arulmurugan *et al*. [11]. This decrease in the lattice constant may be due to change in the cation distribution between A site and B site. in the nano regime [12-14]. However there is an increase in the lattice constant with the increase in the Cd content. This increase in the lattice constant is due to larger ionic radii of the Cd^{2+} (0.97 Å) as compared to Fe^{3+} (0.64 Å) ions [15]. The intensities of the planes (220) and (440) are more sensitive to any change in cation on tetrahedral A sites and octahedral B sites respectively [13, 15]. Cd^{2+} ions and Zn^{2+} ions have chemical affinity towards tetrahedral A sites. Mean while Mn^{2+} and Fe^{3+} ions have, preferences for both tetrahedral A sites and octahedral B sites respectively [14, 16]. Since the X-Ray scattering factor for Cd^{2+} ion is significantly high as compared to those of the other cations, the intensities of the (220) plane and (440) plane increases with increasing Cd^{2+} ion concentration. This shows that Cd^{2+} ions occupy tetrahedral A sites and octahedral B sites in the nano dimension against their chemical preference for A site as observed in bulk samples. Hence there is a small increase in the intensities of (220) and (440) plane. The occupation of Cd^{2+} ion on the octahedral B site forces some of the Fe^{3+} ions to migrate from B site to A site. Hence there is a deviation in the cation distribution from normal in the nano dimension. Figure 2 shows the TEM image of $Mn_{0.5}Zn_{0.3}Cd_{0.2}Fe_2O_4$. It is observed that all the samples are highly homogenous and nearly spherical in shape. The clear SEM image of the sample with x = 0.2 as observed from the Figure 3 reveals that there are no secondary phases. This is supported by the absence of additional peaks in the XRD pattern. The micrograph also shows the presence of more number of smaller grains. Smaller grains have large surface to volume ratio which have a direct effect on the properties of these ferrites.

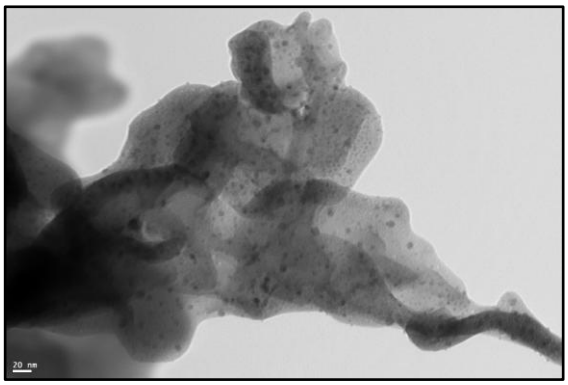

Fig. 2. TEM Image of $Mn_{0.5}\ Zn_{0.3}\ Cd_{0.2}\ Fe_2O_4$.

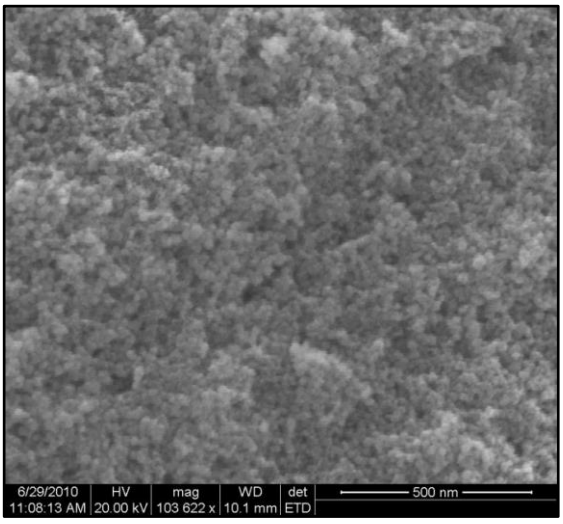

Fig. 3. SEM Image of $Mn_{0.5}\ Zn_{0.3}\ Cd_{0.2}\ Fe_2O_4$.

EPR Spectral studies

The powder EPR spectra of $Mn_{0.5}$ $Zn_{(0.5-x)}Cd_x$ Fe_2O_4 with x= 0.0. 0.1, 0.2 and 0.3 were measured at 9.3 GHz at room temperature and are shown in Figure 4. The EPR of ferrites is important for investigating the magnetic properties of magnetic materials at high frequency because the resonance originates from the interaction between spin and electromagnetic waves. The resonance line width (ΔH), the position corresponding to zero signal (H_o) and the effective g factors are the three parameters that characterize the magnetic properties[17-19]. The effective g factor is determined from the equation

$$g = \frac{h\gamma}{\beta H} \qquad (2)$$

Where h is the Planck's constant, γ is the frequency of the microwave, H is the magnetic field occurring at the maximum resonance and β is the Bohr magneton.

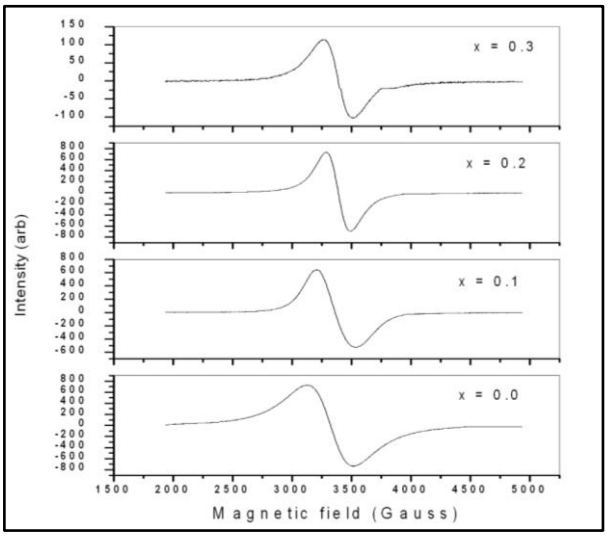

Fig. 4. EPR Spectra for $Mn_{0.5}$ $Zn_{(0.5-x)}Cd_x$ Fe_2O_4 (x = 0.0, 0.1, 0.2, 0.3).

Figure 5 shows the relation between magnetic moment and the resonance field B as a function of Cd content. The resonance field B increases with increase in the Cd content and reaches a maximum for the sample x = 0.2, whereas the magnetic moment decreases with increase in Cd content. This can be attributed to the reason that as the magnetic moment decreases, the internal field also decreases. So to satisfy the relation ω = γH, the resonance field should be high.

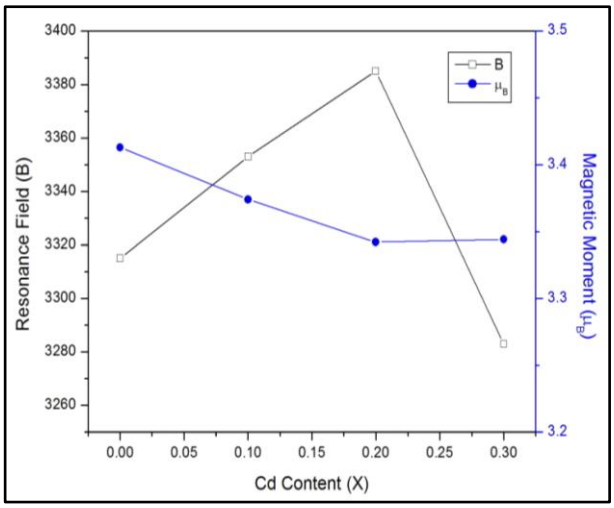

Fig.5. Relation between magnetic moment (μ) and the resonance field (H_R) as a function of Cd content.

The variation of peak to peak line width (ΔH_{pp}) of the EPR signal with Cd content is shown in Figure 6. The line width decreases with increase in the Cd content upto x=0.2. From our earlier studies [12], it was observed that the Cd^{2+} ions occupy both A site and B site in the nano regime. As the Cd content is increased, there is an increase in the occupation of Cd^{2+} ion in the B site. The presence of non-magnetic Cd^{2+} ion in the B site causes a decrease in the magnetization of B site. The occupation of Cd^{2+} ion in the B site forces some of the Fe^{3+} ions to migrate from B site to A site. Hence the magnetization of the A site increases. As a result the net magnetization (M_B-M_A) decreases. This decrease in the magnetization may be the reason for the decrease in the line width.

The super exchange interaction in ferrites is responsible for magnetic ordering within each sub lattice. The interaction between A and B site is strongest in ferrites. As the AB interaction predominate, the spins of A and B site ions in ferrites will be opposite with a resultant magnetic moment equal to the difference between those of A and B site ions [20-22]. It was observed from the Table 2, that the value of g decreases with increasing Cd content up to x = 0.2. This may be due to the decrease in the super exchange interaction between Fe^{2+} and Fe^{3+} at octahedral B

sites. As the Cd content is increased to x=0.3, there is a decrease in the occupation of Cd^{2+} ions in the octahedral B site. Hence there is an increase in the super exchange interaction between Fe^{2+} and Fe^{3+} at octahedral B sites leading to an increase in g value.

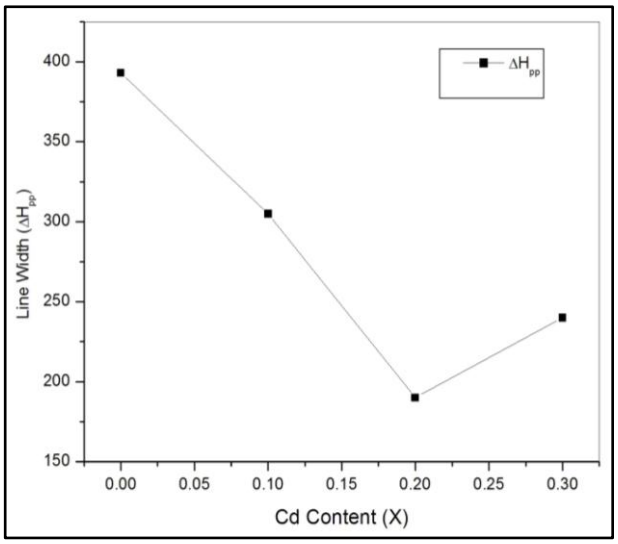

Fig. 6. Variation of line width with Cd content.

The theoretical values of the magnetic moment per formula unit and the experimental values of the magnetic moment is given in Table 2. It was observed that the experimental values of the magnetic moment are lower than the theoretical values. This may be due to occupation of Cd^{2+} ions in the B site. This forces Fe^{3+} ions from B site to A site. As a result, magnetization at B site decreases resulting in overall decrease in the magnetization of the sample. In addition to deviation in cation distribution, the other factors reported in the literature by other researchers may contribute to the reduction of saturation magnetization in nano particles. Coey [23] attributed the smaller value of saturation magnetization in nanoparticles to the existence of random canting of particles surface spins caused by competing antiferromagnetic exchange interactions due to asymmetry in the environment of these spins. Smaller grains have larger surface to volume ratio. Spin disorder from the surface of the nanoparticles increases especially when the surface/volume is large [24, 25]. This spin disorder causes lower magnetization. Surface effects and the occurrence of a glassy state were also reported to be playing an active role in the decline of magnetization value [26].

Table 2. EPR Parameters for the system $Mn_{0.5}Zn_{(0.5-x)}Cd_xFe_2O_4$ (x = 0.0, 0.1, 0.2 and 0.3).

x	Composition	ΔH_{pp} Gauss	Resonance Field(B) Gauss	g_{eff}	Magnetic Moment μ(exp)	Magnetic moment μ(theo)
0.0	$Mn_{0.5}Zn_{0.5}$ Fe_2O_4	393	3315	2.048	3.413	6.322
0.1	$Mn_{0.4}Zn_{0.5}Cd_{0.1}$ Fe_2O_4	305	3353	2.024	3.374	6.058
0.2	$Mn_{0.3}Zn_{0.5}Cd_{0.2}$ Fe_2O_4	190	3385	2.005	3.342	6.005
0.3	$Mn_{0.2}Zn_{0.5}Cd_{0.3}$ Fe_2O_4	240	3283	2.007	3.344	6.370

CONCLUSIONS

Cd substituted Mn-Zn nanoferrites were prepared by co-precipitation method. The X-ray intensity of the (440) plane and (220) plane increases with increasing Cd^{2+} ion concentration. This shows that Cd^{2+} ions occupy both tetrahedral A site and octahedral B sites in the nano dimension. The line width decreases with increase in Cd content. The value of g decreases with increase in the Cd content. This is due to the increase in the super exchange interaction between Fe^{2+} and Fe^{3+} ions at octahedral B sites. Low experimental value of magnetic moment calculated from Electron Paramagnetic Resonance (EPR) spectra confirms the existence of non collinear magnetic structure in the nano regime.

REFERENCES

[1] Rath C., Sahu K. K., Anand S., Date S. K., Mishra N. C., Das R. P., (2004), Preparation and characterization of nanosize Mn-Zn ferrite. *J. Magn. Magn. Mater*. 281: 276-280.

[2] Gul I. H., Ahmed W., Maqsood A., (2008), Electrical and Magnetic characterization of nano Crystalline Ni-Zn ferrite synthesized by co-precipitation route. *J. Magn. Magn. Mater*. 320: 270-275.

[3] Azadmanjiti J., Salehani H. K., Barati M. R., Farzan F., (2007), Preparation and electromagnetic properties of $Ni_{1-x}Cu_xFe_2O_4$ nanoparticles ferrites by sol gel combustion methods. *Mater. Lett*. 61: 84-88.

[4] Wennerstrom H., Soderman O., Olsson U., Lindman B., (1997), Macroemulsion versus microemulsion. *Colloids Surf. A.* 123: 13-16.

[5] Satyanarayana L., Madhusudan Reddy K., Manorama S. V., (2003), Nanosized spinel $NiFe_2O_4$: A novel material for the detection of liquified petroleum gas in air. *Mater. Chem. Phys*. 21: 82-87.

[6] Singh A. K., Goel T. C., Mendiratta R. G., (2004), High performance Ni substituted Mn-Zn ferrites processed by soft chemical technique. *J. Magn. Magn. Mater*. 281: 276-279.

[7] Junior A. F., Lima E. C. de O., Novak M. A., Wells Jr P. R., (2007), Synthesis of nanoparicles of $CoFe_2O_4$ by combustion reaction method. *J. Magn. Magn. Meter*. 308: 198-202.

[8] Rajesh I., Rucha D., Upadhyay R. V, (2009), Low temperature synthesis of nanosized Mn_{1-x} $Cd_xFe_2O_4$,. *Indian J. Pure and Appl. Phys*. 47: 180-185.

[9] Cullity R. D., (1996), Elements of X-ray Diffraction. Addision-Wesley Public Co. INC; 42.

[10] Morrish A. H., Clark P. E., (1975), High-field Mössbauer study of manganese-Zinc ferrites. *Phys. Rev. B*. 11: 278-282.

[11] Arulmurugan R., Jeyadevan B., Vaidyanayhan G., Sendhilnathan S., (2008), Effect of Zinc substitution on Co-Zn and Mn-Zn ferrite nanoparticles prepared by co-precipitation. *J. Magn. Magn. Mater*. 288: 470-477.

[12] Venkataraju C., Sathishkumar G., Sivakumar K., (2011), Effect of Cd on thestructural, magnetic and electrical properties of nanostructured Mn-Zn ferrite. *J. Magn. Magn. Mater*. 323: 1817- 1823.

[13] Ladgaonkar B. P., Vaingainkar A. S., (1998), X-ray diffraction investigation of cation distribution in $CdCu_{1-x}Fe_2O_4$, *Mater. Chem. Phys*. 56: 280-283.

[14] Rajesh I., Rucha D., Upadhyay R. V., (2009), Low temperature synthesis of nano sized $Mn_{(1-x)}$ $Zn_xFe_2O_4$ ferrites and their characterization. *Bull. Mater. Sci*. 32: 141-147.

[15] Narasimhan C. S., Swamy C. S., (1980), Studies on the Solid State Properties of the Solid Solution Systems $MgAl_{(2-x)}$ $FexO_4$. *Physica Status Solidi A.* 59: 817-821.

[16] Vyawahare S. K., Shamkuwar N. R., Madan C. S., (2005), Structural and magnetic properties of $Mn_{(1+x)}Si_xFe_{(1-x)}Cr_{(1-x)}O_4$. *Indian J. Pure and Applied Science*. 43: 545-549.

[17] Shafi K. V. P. M., Gedanken A., Prozorov R., Balogh J., (1988), Sonochemical preparation and size dependent properties of nanostructured $CoFe_2O_4$ particles. *Chem. Mater*. 10: 3445-3451.

[18] Diehl M. R., Yu J. Y., Heath J. R., Held G. A., Doyle H., Sun S. H., Murray C. B., (2001), Crystalline shape and surface anisotropy in two crystal morphologies of superparamagnetic cobalt nanoparticles by ferromagnetic resonance. *J. Phys. Chem. B*. 105: 7913-7919.

[19] Xuebo C., Li G. U., (2005), Spindly cobalt ferrite nanocrystals preparation, characterization and magnetic properties. *Nanotech*. 16: 180-185.

[20] Wiilard M. A. Nakamura Y., Laughlin D. E., Mechenry M. E., (1999), Magnetic properties of ordered and disordered spinel space ferrimagnet. *J. Am. Ceram. Soc*. 82: 3342 – 3346.

[21] Smith J., Wijn H. P. J., (1959), Ferrites, philips technical library, Eindhoven, The Netherlands; .278.

[22] Standley K. J., (1972), Oxide Magnetic Materials, Claredon Press; *Oxford*; 140.

[23] Coey J. M. D, (1971), Noncolinear spin arrangement in ultrafine ferromagnetic crystals. *Phys. Rev. Lett*. 27: 1140-1142.

[24] Pankhrust Q. A., Pollard R. J., (1991), Orgin of the spin canting anomaly in small ferromagnetic particles. *Phys. Rev. Lett*. 67: 248-250.

[25] Venkataraju C., Sathishkumar G., Sivakumar K., (2010), Effect of cation distribution on the structural and magnetic properties of nickel substituted nanosized Mn-Zn ferrite prepared by co-precipitation method. *J. Magn. Magn. Mater*. 322: 230-233.

[26] Garcia del Muro M., Battle X., Labarta A., (1999), Erasing the glassy state in magnetic fine particles. *Phys. Rev*. (B). 59: 13584-13587.

Cite this article as: C. Venkataraju & R. Paulsingh: EPR studies of Cd substituted Mn Zn nanoferrites. *Int. J. Nano Dimens.* 6(3): 255-261, Summer 2015.